UCLA
UCLA Previously Published Works

Title
Lipid Bicelle Micropatterning Using Chemical Lift-Off Lithography

Permalink
https://escholarship.org/uc/item/2rh9h3f6

Journal
ACS Applied Materials & Interfaces, 12(11)

ISSN
1944-8244

Authors
Belling, Jason N
Cheung, Kevin M
Jackman, Joshua A
et al.

Publication Date
2020-03-18

DOI
10.1021/acsami.9b20617

Peer reviewed

eScholarship.org Powered by the California Digital Library
University of California

Author Manuscript

Author Manuscript

Author Manuscript

Author Manuscript

HHS Public Access

Author manuscript

ACS Appl Mater Interfaces. Author manuscript; available in PMC 2020 March 24.

Published in final edited form as:

ACS Appl Mater Interfaces. 2020 March 18; 12(11): 13447–13455. doi:10.1021/acsami.9b20617.

Lipid Bicelle Micropatterning Using Chemical Lift-Off Lithography

Jason N. Belling[1,2], **Kevin M. Cheung**[1,2], **Joshua A. Jackman**[3,4], **Tun Naw Sut**[5], **Matthew Allen**[1,2], **Jae Hyeon Park**[1,2], **Steven J. Jonas**[1,6,7,8], **Nam-Joon Cho**[*,4,5], **Paul S. Weiss**[*,1,2,4,9,10]

[1]California NanoSystems Institute, University of California, Los Angeles, Los Angeles, California 90095, United States

[2]Department of Chemistry and Biochemistry, University of California, Los Angeles, Los Angeles, California 90095, United States

[3]School of Chemical Engineering, Sungkyunkwan University, Suwon 16419, Republic of Korea

[4]SKKU-UCLA-NTU Precision Biology Research Center, Sungkyunkwan University, Suwon 16419, Republic of Korea

[5]School of Materials Science and Engineering, Nanyang Technological University, Singapore, 639798, Singapore

[6]Department of Pediatrics, David Geffen School of Medicine, University of California, Los Angeles, Los Angeles, California 90095, United States

[7]Children's Discovery and Innovation Institute, University of California, Los Angeles, Los Angeles, California 90095, United States

[8]Eli & Edythe Broad Center of Regenerative Medicine and Stem Cell Research, University of California, Los Angeles, Los Angeles, California 90095, United States

[9]Department of Bioengineering, University of California, Los Angeles, Los Angeles, California 90095, United States

[10]Department of Materials Science and Engineering, University of California, Los Angeles, Los Angeles, California 90095, United States

Abstract

Supported lipid membranes are versatile biomimetic coatings for the chemical functionalization of inorganic surfaces. Developing simple and effective fabrication strategies to form supported lipid membranes with micropatterned geometries is a long-standing challenge. Herein, we demonstrate how the combination of chemical lift-off lithography (CLL) and easily prepared lipid bicelle nanostructures can yield micropatterned, supported lipid membranes on gold surfaces with high

[*]**Corresponding Authors**: njcho@ntu.edu.sg, psw@cnsi.ucla.edu.

Supporting Information Available

The Supporting Information is available free of charge on the ACS Publications website at DOI: 10.1021/acs.

Additional details about the materials and methods, including reagents, patterning steps, instrumental tools, and experimental characterization.

Author Manuscript Author Manuscript Author Manuscript Author Manuscript

pattern resolution, conformal character, and biofunctionality. Using CLL, we functionalized gold surfaces with patterned arrays of hydrophilic and hydrophobic self-assembled monolayers (SAMs). Time-lapse fluorescence microscopy imaging revealed that lipid bicelles adsorbed preferentially onto the hydrophilic SAM regions while there was negligible lipid adsorption onto the hydrophobic SAM regions. Functional receptors could be embedded within the lipid bicelles, which facilitated selective detection of receptor-ligand binding interactions in a model streptavidin-biotin system. Quartz crystal microbalance-dissipation measurements further identified that lipid bicelles adsorb irreversibly and remain intact on top of the hydrophilic SAM regions. Taken together, our findings indicate that lipid bicelles are useful lipid nanostructures for reproducibly assembling micropatterned, supported lipid membranes with precise pattern fidelity.

Graphical Abstract

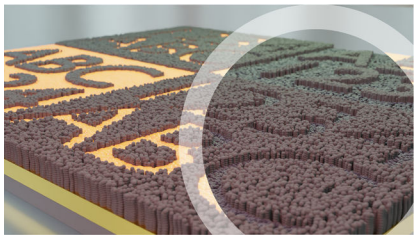

Keywords

soft lithography; self-assembled monolayer; micropatterning; supported lipid bilayer; bicelle

Introduction

Microscale patterning of solid-supported lipid membranes is a challenging task that involves controlling the self-assembly pathway of adsorbing lipid molecules on a material surface along with precise chemical functionalization of the target interface. While it is possible to tether patterned arrays of three-dimensional (3D) lipid vesicles on solid supports,[1] most studies focus on two-dimensional (2D) lipid membrane architectures, such as supported lipid bilayers (SLBs), because they provide conformal coatings that are well-suited for a wide range of sensor and biotechnology applications.[2–5]

Early work on SLB micropatterning focused on silica-based surfaces on which solution-phase lipid vesicles typically adsorb and rupture spontaneously to form SLBs.[6–8] These strategies dealt with pre-installing material barriers to inhibit vesicle adsorption and/or SLB formation in specific locations on the target surface.[9] For example, Groves *et al.* used photolithographic methods to form grids of photoresist, aluminum oxide, or gold on oxidized silicon substrates where adsorbing vesicles would fuse and rupture on oxidized silicon while the grid regions inhibited vesicle adsorption and/or SLB formation.[10,11] Kung *et al.* expanded on this concept to micropattern SLBs on glass surfaces by applying soft lithographic approaches with protein-based coatings.[12] Other work has also shown that functionalizing silica-based surfaces with hydrophilic polymers can enable selective SLB patterning across the nano- to micron scales by employing the vesicle fusion method.[13–16]

Author Manuscript Author Manuscript Author Manuscript Author Manuscript

In marked contrast to silica surfaces, vesicles typically adsorb but do *not* rupture on gold surfaces,[6,17] thereby limiting opportunities to form micropatterned SLBs based on the aforementioned design principles. Rather, Jenkins *et al.* demonstrated how microcontact printing of hydrophilic self-assembled monolayers (SAMs) on gold surfaces promoted tethered SLB formation from adsorbing vesicles.[18,19] The structural conversion of adsorbed vesicles into a SLB on hydrophilic SAMs entails complex formation processes that depend on the pattern geometry.[20] Using microcontact printing, Strulson and Maurer demonstrated the formation of patterned SLBs on tetra(ethylene glycol) SAMs from adsorbing vesicles whereby lipid monolayers formed on reinserted hydrophobic SAM regions.[21] Notably, the SLB formation process depended on vesicle adsorption at the interface between the hydrophilic and hydrophobic SAM regions.[22] Altogether, these findings support that micropatterning of supported lipid membranes on gold surfaces is possible, and open the door to exploring new patterning strategies and lipid membrane architectures that can be used for a variety of applications. For example, patterned arrays of SLB-functionalized gold surfaces would be useful detection platforms for electrochemical or plasmonic characterization of important biomembrane-related processes such as lipid-receptor interactions involved in cell signaling and the mimicking of T-cell immunological synapses.[23,24] Moreover, control of the physicochemical properties of patterned membranes can enable selective cell capture for cell-based assays and the monitoring of cell behavior in controlled microenvironments such as cellular differentiation.[25.26]

Herein, we report a robust and efficient strategy to micropattern a well-packed, adsorbed layer of 2D lipid bicelles on chemically functionalized gold surfaces. Our approach combines chemical lift-off lithography (CLL) – a soft-lithographic method to pattern hydrophilic and hydrophobic SAMs on gold and other surfaces using plasma-activated polydimethylsiloxane (PDMS) stamps[27–32] – and lipid bicelles, which are easily prepared, 2D lipid nanostructures that readily adsorb onto hydrophilic surfaces.[33–35] Importantly, the subtractive patterning process of CLL enables high-resolution patterning with sharp borders while avoiding the challenges of conventional soft lithographic methods (*e.g.*, microcontact printing) such as lateral diffusion of molecular inks.[36–39] Using fluorescence microscopy imaging and quartz crystal microbalance-dissipation (QCM-D) measurements, we demonstrate how bicelles are versatile lipid nanostructures for assembling supported lipid membranes with conformal character and high pattern fidelity, along with excellent utility for studying membrane-associated biomacromolecular interactions such as ligand-receptor binding.

Results and Discussion

Lipid self-assembly on solid supports is strongly linked to the physicochemical properties of the target material surface.[8,40] When lipid nanostructures (*e.g.*, bicelles and/or vesicles) interact with hydrophilic surfaces, lipid adsorption typically occurs while hydrophobic surfaces can inhibit lipid adsorption, depending on the surface free energy[41] and lipid-surface adhesion strength.[42] The adhesion is mainly affected by the energetic mismatch between the hydrophobic surface and hydrophilic lipid headgroups and also depends on the adsorption footprint of a contacting lipid nanostructure.[42] Thus, we developed a CLL-based micropatterning strategy that utilizes a combination of hydrophilic and hydrophobic SAMs

Author Manuscript Author Manuscript Author Manuscript Author Manuscript

to control supported lipid membrane formation on gold surfaces spatially. The fabrication steps are outlined in Figure 1. Bare gold surfaces were incubated with an ethanolic solution of mercaptoundecanol (HSC11-OH) to form a hydrophilic SAM. Selective removal of HSC11-OH monolayer regions was then conducted by contacting and then removing a patterned oxygen plasma-activated PDMS stamp from the functionalized gold surface. The treated surface was next incubated with an ethanolic solution of octadecanethiol (HSC18) so that these hydrophobic molecules are covalently attached within the lifted-off regions. The resulting surface is composed of a patterned combination of hydrophilic and hydrophobic SAMs of HSC11-OH and HSC18 molecules, respectively. The hydrophilic molecule, HSC11-OH, possesses suitable chemical properties for chemical lift-off while the hydrophobic molecule, HSC18, can form well-packed SAMs and can backfill void regions while preserving the target pattern regions of covalently attached HSC11-OH molecules.[29] Successful lift-off of HSC11-OH SAMs and backfilling with HSC18 SAMs in target patterned regions was tested and confirmed by atomic force microscopy (AFM) characterization in height and adhesion force modes (Figure S1). Based on this platform design, we were able to achieve selective adsorption of the lipid bicelle nanostructures onto the hydrophilic SAMs in order to form a micropatterned supported lipid membrane.

As a first step, we conducted fluorescence microscopy experiments to investigate the adsorption of fluorescently labeled bicelles and vesicles – two widely studied classes of lipid nanostructures – onto functionalized gold surfaces with different pattern geometries (Figure 2). While gold surfaces can quench fluorescent molecules in close proximity to the substrate, the quenching effect is distance dependent and SAMs have been shown to mitigate fluorescence quenching significantly, as spacers from the surface.[43,44] Thus, we were able to observe bicelle and vesicle adsorption onto SAM-functionalized surfaces with time-lapse monitoring. The bicelles were composed of a mixture of long-chain 1,2-dioleoyl-*sn*-glycero-3-phosphocholine (DOPC) and short-chain 1,2-dihexanoyl-*sn*-glycero-3-phosphocholine (DHPC) lipids with a q-ratio of 0.25 (*i.e.*, ratio of long-chain to short-chain phospholipids). Vesicles used in these studies were composed of an equivalent concentration of the DOPC lipid alone. Both types of lipid mixtures also contained a small amount of 1,2-dipalmitoyl-*sn*-glycero-3-phos-phoethanolamine-*N*-(lissamine rhodamine B sulfonyl) lipid to facilitate fluorescence visualization. Both bicelles and vesicles were prepared in 10 mM Tris buffer [pH 7.5] with 150 mM NaCl by the freeze-thaw-vortexing method and had similar hydrodynamic diameters of around 400 nm (Figure S2).[45]

The lipid nanostructures were incubated with the functionalized gold surface for 45 min before a buffer washing step, followed by fluorescence microscopy imaging. As shown in Figure 2A, the lipid bicelles formed high-resolution micropatterns whereby the fluorophore-enriched red regions correspond to supported lipid membranes on top of hydrophilic SAM regions while the fluorophore-deficient black regions depict hydrophobic SAM regions where the bicelles did not adsorb. Supported lipid membranes formed according to the underlying patterned SAM features with dimensions as small as 5 μm. Well-packed lipid bicelle adlayers with a conformal appearance were observed on patterns with different scales and geometries. By contrast, the lipid vesicles were less effective at forming micropatterned, supported lipid membranes (Figure 2B). The lipid vesicles appeared to adsorb preferentially onto the hydrophilic SAM regions, however, the deposition process resulted in more

Author Manuscript Author Manuscript Author Manuscript Author Manuscript

disordered adlayers with non-uniform coating appearances, and there was also a moderate level of nonspecific vesicle adsorption on the hydrophobic SAM regions as well.

Using time-lapse fluorescence microscopy imaging, we further investigated the adsorption kinetics of lipid bicelles onto chemically functionalized gold surfaces (Figure 3). Within the first 2 min, the fluorescently labeled bicelles adsorbed preferentially onto the hydrophilic SAM regions, while some defects were initially present along with some nonspecific bicelle adsorption onto the hydrophobic SAM regions. Over time, the defects vanished and there was also increased resolution such that the bicelle pattern mirrored the underlying pattern of hydrophilic and hydrophobic SAM regions. The fluorescence intensity becomes more uniform within the bicelle-patterned hydrophilic regions, indicating that bicelle adsorption on the hydrophilic SAM regions continued until reaching saturation after *ca.* 20 min. Importantly, the pattern resolution remained stable for at least 24 h and the hydrophobic SAM regions acted as barriers to keep the supported lipid membranes contained within the hydrophilic SAM regions.

In addition to characterizing the formation process, we also investigated the functionality of the micropatterned, supported lipid membranes by incorporating 1 mol% of 1,2-dioleoyl-*sn*-glycero-3-phosphoethanolamine-*N*-(cap biotinyl) (Biotin-PE) lipid into the bicelle mixture in order to study ligand-receptor interactions (Figure 4). In this case, the supported lipid membranes were fabricated without fluorescently labeled phospholipid and the subsequent binding of fluorescently labeled streptavidin to the biotinylated lipids was detected by time-lapse fluorescence microscopy imaging, as outlined in Figure 4A. The binding scheme was highly specific as negligible streptavidin binding occurred on chemically functionalized gold surfaces without supported lipid membrane coating and on bicelle-patterned surfaces that did not contain biotinylated lipid (Figures 4B,C). In the case of the bicelle-patterned surface that included biotinylated lipid, streptavidin binding to the bicelle pattern was detected within 10 min – as indicated by the fluorescence signal emitted by labeled streptavidin molecules (Figure 4D). Streptavidin binding was concentrated in the bicelle-coated regions on top of the hydrophilic SAM regions. Even without a blocking protein layer (*e.g.*, bovine serum albumin) on top of the hydrophobic SAMs, nonspecific streptavidin binding was minimal. Within 20 min, the amount of bound streptavidin within the bicelle-coated areas reached stable levels, demonstrating that membrane-associated receptors can be included in the bicelle mixtures and functionally incorporated within the micropatterned, supported lipid membranes.

The aforementioned results demonstrate that lipid bicelles selectively adsorb onto hydrophilic SAM-functionalized gold surfaces, which correspond to C11-OH monolayers based on our platform design, and form well-packed adlayers. In order to characterize the bicelle adlayer properties, we conducted QCM-D experiments in order to track bicelle and vesicle adsorption onto bare and HSC11-OH-functionalized gold surfaces (Figure 5). In the QCM-D measurements, resonance frequency (Δf) and energy dissipation (ΔD) shifts arising from lipid adsorption reflect changes in the mass and viscoelastic properties of the adlayer, respectively.[46] On bare gold surfaces, lipid bicelles and vesicles exhibited similar adsorption kinetic profiles that are consistent with adsorption of intact bicelles or vesicles in the two respective cases (Figure 5A). Equivalent Δf shifts of *ca.* −15 Hz were observed, while 3×

Author Manuscript Author Manuscript Author Manuscript Author Manuscript

larger ΔD shifts were observed for vesicles (3×10^{-6} *vs* 1×10^{-6}) (Figure 5B,C). The larger ΔD shift of adsorbed vesicles is likely due to the geometrical differences between the nearly planar, 2D bicelles and 3D spherical vesicles that have more hydrodynamically coupled solvent per adsorption and, hence, contribute to a larger viscoelastic response than bicelles.[47] Time-independent analyses[48] of the Δf *vs* ΔD signals for the bicelle and vesicle adsorption cases are consistent with bicelles attaching more rigidly to the bare gold surface (Figure S3). Together, the data support that bicelles adsorb to a greater extent than vesicles when taking into account the respective hydrodynamic factors.

On HSC11-OH-functionalized gold surfaces, it was also observed that lipid bicelles and vesicles adsorb and remain intact without rupturing (Figure 5D). Similar results have been reported for vesicle adsorption onto hydrophilic SAM surfaces,[18] while the QCM-D measurements in our case further revealed that bicelle adsorption was appreciably quicker than vesicle adsorption, which did not reach equilibrium on the measurement time scale. In addition, bicelle adsorption onto HSC11-OH-functionalized gold surfaces was more favorable than on bare gold surfaces, as indicated by larger Δf and ΔD shifts of *ca.* −30 Hz and 4×10^{-6}, respectively (Figures 5E,F). The adsorption kinetics and final QCM-D shifts indicate that the adsorbed bicelles remain intact on the HSC11-OH monolayer to form a well-packed adlayer.

In contrast, vesicle adsorption onto HSC11-OH-functionalized gold surfaces yielded significantly larger Δf and ΔD shifts of around −120 Hz and 40×10^{-6}, respectively, than on bare gold surfaces. The ΔD shift for vesicle adsorption in this case was more than 10× larger than the corresponding signal on bare gold surfaces. The large measurement responses associated with vesicle adsorption are indicative of weak vesicle adhesion to the HSC11-OH monolayer whereby adsorbed vesicles experience minimal substrate-induced deformation and hence contribute to a larger viscoelastic response.[49] This finding helps to explain why lipid vesicles were less effective than bicelles in forming micropatterned, supported lipid membranes.

We also characterized lipid bicelle and vesicle adsorption onto HSC18-functionalized gold surfaces. The QCM-D data showed that there was minimal bicelle adsorption onto the HSC18-functionalized gold surface (−1.25 ± 2.5 Hz), which is consistent with the fluorescence microscopy results. Of note, DOPC/DHPC bicelles are equilibrium-phase structures that co-exist with free DHPC molecules in bulk solution,[50] so we also measured free DHPC lipid adsorption onto the HSC18-functionalized gold surfaces and observed similar Δf shifts as in the bicelle case (Figure S4). Taken together, the data support that DHPC lipid molecules are the main component in the bicelle system that adsorbs to the HSC18 monolayer and the complex, two-step interaction kinetics further indicate that DHPC molecules intercalate within the HSC18 monolayer. Thus, in the bicelle case, the DHPC molecules appear to play an important role in passivating nonspecific adsorption on the HSC18 monolayer regions, as evidenced by the negligible levels of bicelle and streptavidin adsorption described above (*cf.* Figures 2–4).

On the other hand, for vesicle adsorption onto HSC18-functionalized surfaces, we observed larger Δf shifts of around −11 ± 2 Hz that did not reach equilibrium over a 30-min time

Author Manuscript Author Manuscript Author Manuscript Author Manuscript

interval. This observation agrees well with our fluorescence microscopy results, which showed a moderate degree of nonspecific vesicle adsorption onto HSC18-functionalized surfaces. It has also been reported that lipid vesicle interaction processes with hydrophobic SAMs can take a long time to reach equilibrium, up to several hours and depend on the specific system (*e.g.*, SAM molecular packing, vesicle preparation, vesicle size), while our incubation protocol occurs on much shorter time scales.[51–53] Taken together, the QCM-D data support that both types of lipid nanostructures – bicelles and vesicles – adsorb onto bare and hydrophilic HSC11-OH-functionalized gold surfaces. The bicelle system enables the formation of well-packed adlayers on the hydrophilic SAM region while also inhibiting nonspecific adsorption on the HSC18-functionalized gold surface (hydrophobic SAM region) due to DHPC molecular passivation along with the large contacting surface area of an adsorbing bicelle.

Conclusions and Outlook

In this work, we have demonstrated that, when combined with CLL fabrication capabilities, lipid bicelles are useful lipid nanostructures for preparing supported lipid membranes with micropatterned geometries. From a materials design perspective, the bicelles have three key advantages: First, they are easily prepared, requiring only aqueous hydration followed by a few cycles of freeze-thaw-vortexing. Second, the bicelles have 2D disk architectures that are well-suited for forming non-fouling, conformal layers without requiring SLB formation. Third, the high surface-area-to-volume ratios of adsorbed lipid bicelles facilitate large contact areas that support firm, irreversible attachment to hydrophilic SAMs while helping to minimize attachment to hydrophobic SAMs in tandem with DHPC molecular passivation. By contrast, the packing constraints and smaller surface-area-to-volume ratios of adsorbing vesicles result in non-conformal layers and less discrimination between hydrophilic and hydrophobic SAMs. As such, our findings provide strong experimental evidence supporting the merits of lipid bicelles as macromolecular building blocks for the fabrication of micropatterned, supported lipid membrane platforms. Considering that lipid bicelles are widely used to reconstitute transmembrane proteins in membranous environments, we anticipate that these fabrication capabilities could be broadly useful for developing micropatterned arrays of supported lipid membranes that incorporate membrane proteins and other membrane-associated entities for applications such as pharmacological drug testing and high-throughput screening assays.

Materials and Methods

Chemical Lift-Off Lithography.

Siloxyl groups were formed on PDMS stamps by exposure of molded features to oxygen plasma (Harrick Plasma, Ithaca, NY, USA) for 40 s at a power of 18 W with a chamber pressure of 10 psi. By contacting the oxygen plasma-treated PDMS stamps to an underlying HSC11-OH SAM, a condensation reaction occurs, yielding covalent binding between the distal hydroxyl groups of HSC11-OH SAM molecules and the siloxyl groups on the patterned PDMS surface. When the PDMS stamp was retracted from the gold surface, strong bonding between these two interfaces led to the subsequent lift-off of HSC11-OH molecules

Author Manuscript Author Manuscript Author Manuscript Author Manuscript

and gold atoms. The exposed regions of bare gold surface were subsequently functionalized by incubating the substrate in a 5 mM ethanolic solution of HSC18 molecules for 1 h, resulting in the formation of a functionalized gold surface with well-defined regions of hydrophilic and hydrophobic SAMs.

Lipid Nanostructure Preparation.

To fabricate lipid bicelles, 1 mg each of DOPC and DHPC phospholipids in chloroform were dispensed individually into separate glass test tubes and the chloroform solvent was evaporated by rotating the tubes under a gentle stream of nitrogen gas to form dry lipid films, followed by placing the tubes in a vacuum desiccator overnight. Then, the dry DOPC lipid film was hydrated in an aqueous buffer (10 mM Tris [pH 7.5] with 150 mM NaCl) in order to prepare a 63 μM DOPC lipid stock solution. The DOPC lipid solution was then used to hydrate the DHPC lipid film so that the final concentration of DHPC lipid was 252 μM. As a result, the molar ratio (“q-ratio”) between DOPC long-chain phospholipids and DHPC short-chain phospholipids was 0.25. After preparing the DOPC/DHPC lipid mixture, the solution was plunged into liquid nitrogen for 1 min, followed by 5 min incubation in a 60 °C water bath and subsequent vortexing for 30 s. This freeze-thaw-vortex cycle was repeated a total of five times. The DOPC lipid vesicles were also prepared using lipid hydration and freeze-thaw-vortex cycling as described above with DOPC lipid concentration fixed at 63 μM. To prepare fluorescently labelled bicelles and vesicles, the initially prepared DOPC lipid stock solution contained 0.5 mol% of fluorescently labelled RhoPE lipid. To prepare biotinylated lipid-containing bicelles, the initially prepared DOPC lipid stock solution contained 1 mol% of Biotin-PE lipid.

Lipid Nanostructure Patterning.

Lipid bicelle and vesicle solutions were incubated with the pre-patterned SAM surface for 45 min under ambient conditions, and then the surface was rinsed with buffer a total of three times to form supported lipid membranes in the hydrophilic SAM regions. The patterned lipid-SAM substrates were kept hydrated during rinsing cycles to prevent delamination of the lipid layer.

Biotin-Streptavidin Binding Experiments.

After patterning the SAM-functionalized substrate with biotinylated lipid-containing bicelles, the solution was carefully exchanged with aqueous buffer (10 mM Tris [pH 7.5] with 150 mM NaCl) using a 1000 μL pipette. Next, fluorescently labeled streptavidin molecules, at a concentration of 17 nM in equivalent buffer, were incubated with the substrate for 45 min at room temperature. Appropriate control experiments without biotinylated lipid and without supported lipid membranes were conducted to verify the binding specificity of the biotin-streptavidin interaction.

Fluorescence Microscopy.

Epifluorescence microscopy experiments were performed using an AxioZ1 Observer fluorescence microscope (Carl Zeiss AG, Oberkochen, Germany) with LD Plan-Neofluar 10×/0.3 and 20×/0.4 objectives. Images were acquired using a 545/25 bandpass excitation

Author Manuscript Author Manuscript Author Manuscript Author Manuscript

filter, a FT 570 beam splitter, and a 605/70 bandpass emission filter (43 HE DsRed filter set).

Quartz Crystal Microbalance-Dissipation (QCM-D).

Lipid adsorption kinetics were monitored using a Q-Sense E4 instrument (Biolin Scientific AB, Stockholm, Sweden). Gold-coated QCM-D sensor chips (QSX 301, Biolin Scientific AB) were used for all experiments and were washed with ethanol and water, dried with nitrogen gas, and then treated with oxygen plasma for 1 min in a plasma cleaner (PDC-002, Harrick Plasma, Ithaca, NY). The sensor chips were either used as-is or next functionalized with a hydrophilic SAM layer by immersing the sensor chips in a 1 mM ethanolic solution of HSC11-OH molecules for 1 h at room temperature. After incubation, the SAM-functionalized sensor chips were rinsed with ethanol before nitrogen gas drying. After assembling bare gold or SAM-functionalized sensor chips within the QCM-D measurement chamber, a baseline signal in aqueous buffer (10 mM Tris [pH 7.5] with 150 mM NaCl) was first established. Then, lipid bicelles or vesicles (63 μM DOCP lipid concentration) in equivalent buffer were injected into the measurement chamber under continuous flow conditions at a volumetric rate of 50 μL/min, as controlled by a peristaltic pump (Reglo Digital, Ismatec, Cole-Parmer GmbH, Wertheim, Germany). Experimental data were collected and processed using the Q-Soft and Q-Tools software packages, respectively, from Biolin Scientific AB. The reported data were collected at the 5^{th} overtone and the frequency shifts were normalized according to the overtone number.

Dynamic Light Scattering (DLS).

The size distribution of lipid bicelles and vesicles was measured by the DLS technique using a 90Plus particle size analyzer instrument (Brookhaven Instruments Corporation, Holtsville, NY) with a 658-nm monochromatic laser. The scattered light was measured perpendicular to the sample. The intensity-weighted size distribution of the vesicles was recorded based on an autocorrelation function, which correlates fluctuations in the scattered light intensity with respect to time[54] and is obtained using Particle Sizing software (Brookhaven Instruments Corporation). The mean hydrodynamic diameter and standard deviation of the bicelle and vesicle sizes are reported for N=5.

Supplementary Material

Refer to Web version on PubMed Central for supplementary material.

Acknowledgments

We thank Prof. Anne Andrews (UCLA) for helpful discussions on chemical patterning and chemical lift-off lithography. We thank Prof. Zoran Galic (UCLA) for providing access to a fluorescence microscope instrument and Dr. Adam Z. Stieg (UCLA) for discussions on lipid surface characterization. This work was supported by a National Research Foundation Proof-of-Concept Grant (NRF2015NRF-POC001-019), the Creative Materials Discovery Program through the National Research Foundation of Korea (NRF) that is funded by the Ministry of Science, ICT, and Future Planning (2016M3D1A1024098), NIH/NCATS UCLA CTSI Grant Number KL2TR001882, and the National Institute on Drug Abuse (DA045550). J.N.B. thanks the NIH for a predoctoral fellowship; research reported in this publication was supported by the National Heart, Lung, and Blood Institute of the National Institutes of Health under Award Number F31HL149356. K.M.C. thanks the Department of Chemistry and Biochemistry at UCLA for a SG fellowship. P.S.W. and S.J.J. thank additional support and seed funding provided through a UCLA David Geffen School of Medicine Regenerative Medicine Theme Award. S.J.J. is

Author Manuscript Author Manuscript Author Manuscript Author Manuscript

supported by is supported by the NIH Common Fund through a NIH Director's Early Independence Award co-funded by the National Institute of Dental and Craniofacial Research and Office of the Director, NIH under award number DP5OD028181. S.J.J. also wishes to acknowledge Young Investigator Award funds from the Alex's Lemonade Stand Foundation for Childhood Cancer Research, the Hyundai Hope on Wheels Foundation for Pediatric Cancer Research, and the Tower Cancer Research Foundation.

References

(1). Brigitte L; Didier F; Indriati P; Fredrik H; Janos V Micropatterning of DNA-Tagged Vesicles. Langmuir 2004, 20, 11348–11354. [PubMed: 15595756]

(2). Castellana ET; Cremer PS Solid Supported Lipid Bilayers: From Biophysical Studies to Sensor Design. Surf. Sci. Rep 2006, 61, 429–444.

(3). Chan Y-HM; Boxer SG Model Membrane Systems and Their Applications. Curr. Opin. Chem. Biol 2007, 11, 581–587. [PubMed: 17976391]

(4). Bally M; Bailey K; Sugihara K; Grieshaber D; Vörös J; Städler B Liposome and Lipid Bilayer Arrays Towards Biosensing Applications. Small 2010, 6, 2481–2497. [PubMed: 20925039]

(5). Hardy GJ; Nayak R; Zauscher S Model Cell Membranes: Techniques To Form Complex Biomimetic Supported Lipid Bilayers *via* Vesicle Fusion. Curr. Opin. Colloid Interface Sci 2013, 18, 448–458. [PubMed: 24031164]

(6). Keller CA; Kasemo B Surface Specific Kinetics of Lipid Vesicle Adsorption Measured with a Quartz Crystal Microbalance. Biophys. J 1998, 75, 1397–1402. [PubMed: 9726940]

(7). Cremer PS; Boxer SG Formation and Spreading of Lipid Bilayers on Planar Glass Supports. J. Phys. Chem. B 1999, 103, 2554–2559.

(8). Biswas KH; Jackman JA; Park JH; Groves JT; Cho N-J Interfacial Forces Dictate the Pathway of Phospholipid Vesicle Adsorption onto Silicon Dioxide Surfaces. Langmuir 2018, 34, 1775–1782. [PubMed: 29281791]

(9). Groves JT; Ulman N; Cremer PS; Boxer SG Substrate-Membrane Interactions: Mechanisms for Imposing Patterns on a Fluid Bilayer Membrane. Langmuir 1998, 14, 3347–3350.

(10). Groves JT; Ulman N; Boxer SG Micropatterning Fluid Lipid Bilayers on Solid Supports. Science 1997, 275, 651–653. [PubMed: 9005848]

(11). Groves JT; Boxer SG Micropattern Formation in Supported Lipid Membranes. Acc. Chem. Res 2002, 35, 149–157. [PubMed: 11900518]

(12). Kung L; Kam L; Hovis J; Boxer SG Patterning Hybrid Surfaces of Proteins and Supported Lipid Bilayers. Langmuir 2000, 16, 6773–6776.

(13). Morigaki K; Kiyosue K; Takahisa T Micropatterned Composite Membranes of Polymerized and Fluid Lipid Bilayers. Langmuir 2004, 18, 7729–7735.

(14). Daniel C; Sohn K; Mates T; Kramer E; Rädler J; Sackmann E; Nickel B; Andruzzi L Structural Characterization of an Elevated Lipid Bilayer Obtained by Stepwise Functionalization of a Self-Assembled Alkenyl Silane Film. Biointerphases 2007, 2, 109–118. [PubMed: 20408645]

(15). Tan C; Craighead H Surface Engineering and Patterning Using Parylene for Biological Applications. Materials 2010, 3, 1803–1832.

(16). Pla-Roca M; Isa L; Kumar K; Reimhult R Selective (Bio)Functionalization of Solid-State Nanopores. ACS Appl. Mater. Interfaces 2015, 16, 6773–6776.

(17). Towns EN; Parikh AN; Land DP Influence of Vesicle Size and Aqueous Solvent on Intact Phospholipid Vesicle Adsorption on Oxidized Gold Monitored using Attenuated Total Reflectance Fourier Transform Infrared Spectroscopy. J. Phys. Chem. C 2015, 119, 2412–2418.

(18). Jenkins ATA; Bushby RJ; Boden N; Evans SD; Knowles PF; Liu Q; Miles RE; Ogier SD Ion-Selective Lipid Bilayers Tethered to Microcontact Printed Self-Assembled Monolayers Containing Cholesterol Derivatives. Langmuir 1998, 14, 4465–4678.

(19). Jenkins ATA; Boden N; Bushby RJ; Evans SD; Knowles PF; Miles RE; Ogier SD; Schönherr H; Vancso GJ Microcontact Printing of Lipophilic Self-Assembled Monolayers for the Attachment of Biomimetic Lipid Bilayers to Surfaces. J. Am. Chem. Soc, 1999, 121, 5274–5280.

Author Manuscript Author Manuscript Author Manuscript Author Manuscript

(20). Jenkins ATA; Bushby RJ; Evans SD; Knoll W; Offenhäusser A; Ogier SD Lipid Vesicle Fusion on μCP Patterned Self-Assembled Monolayers: Effect of Pattern Geometry on Bilayer Formation. Langmuir 2002, 18, 3176–3180.

(21). Strulson MK; Maurer JA Microcontact Printing for Creation of Patterned Lipid Bilayers on Tetraethylene Glycol Self-Assembled Monolayers. Langmuir 2011, 27, 12052–12057. [PubMed: 21866896]

(22). Strulson MK; Maurer JA Mechanistic Insight into Patterned Supported Lipid Bilayer Self-Assembly. Langmuir 2012, 28, 13652–13659. [PubMed: 22935058]

(23). Coyle MP; Xu Q; Chiang S; Francis MB; Groves JT DNA-Mediated Assembly of Protein Heterodimers on Membrane Surfaces. J. Am. Chem. Soc 2013, 135, 5012–5016 [PubMed: 23530555]

(24). Taylor M; Husain K; Gartner Z; Satyajit M; Vale R A DNA-Based T Cell Receptor Reveals a Role for Receptor Clustering in Ligand Discrimination. Cell 2017, 23, 108–119.

(25). Jung DR; Kapur R; Giuliano KA; Mrkisch M; Craighead HG; Taylor DL Topographical and Physicochemical Modificationof Material Surface to Enable Patterning of Living Cells. Crit. Rev. Biotechnol 2001, 21, 111–154. [PubMed: 11451046]

(26). Biswas K; Groves J Hybrid Live Cell–Supported Membrane Interfaces for Signaling Studies. Annu. Rev. Biophys 2019, 48, 537–562. [PubMed: 30943043]

(27). Liao W-S; Cheunkar S; Cao HH; Bednar HR; Weiss PS; Andrews AM Subtractive Patterning *via* Chemical Lift-Off Lithography. Science 2012, 337, 1517–1521. [PubMed: 22997333]

(28). Xu X; Yang Q; Cheung KM; Zhao C; Wattanatorn N; Belling JN; Abendroth JM; Slaughter LS; Mirkin CA; Andrews AM; Weiss PS Polymer-Pen Chemical Lift-Off Lithography. Nano Lett. 2017, 17, 3302–3311. [PubMed: 28409640]

(29). Slaughter LS; Cheung KM; Kaappa S; Cao HH; Yang Q; Young TD; Serino AC; Malola S; Olson JM; Link S; Häkkinen H; Andrews AM; Weiss PS Patterning of Supported Gold Monolayers via Chemical Lift-Off Lithography. Beilstein J. Nanotechnol 2017, 8, 2648–2661. [PubMed: 29259879]

(30). Chen CY; Li HH; Wang CM; Lin LE.; Hsu CC; Liao WS Finely Tunable Surface Wettability by Two-Dimensional Molecular Manipulation. ACS Appl. Mater. Interfaces 2018, 10, 41814–41823 [PubMed: 30412374]

(31). Chen CY; Wang CM; Liao WS A Special Connection between Nanofabrication and Analytical Devices: Chemical Lift-Off Lithography. Bull. Chem. Soc. Jpn 2019, 48, 600–607

(32). Cheung KM; Stemer DM; Zhao C; Young T; Belling JN;Andrews AM; Weiss PS Chemical Lift-Off Lithography of Metal and Semiconductor Surfaces. ACS Appl. Materials Lett 2019, 1, 76–83

(33). Zeineldin R; Last JA; Slade AL; Ista LK; Bisong P; O'Brien MJ; Brueck SRJ; Sasaki DY; Lopez GP Using Bicellar Mixtures To Form Supported and Suspended Lipid Bilayers on Silicon Chips. Langmuir 2006, 22, 8163–8168. [PubMed: 16952257]

(34). Kolahdouzan K; Jackman JA; Yoon BK; Kim MC; Johal MS; Cho N-J Optimizing the Formation of Supported Lipid Bilayers from Bicellar Mixtures. Langmuir 2017, 33, 5052–5064. [PubMed: 28457139]

(35). Sut TN; Jackman JA; Yoon BK; Park S; Kolahdouzan K; Ma GJ; Zhdanov VP; Cho N-J Influence of NaCl Concentration on Bicelle-Mediated SLB Formation. Langmuir 2019, 35, 10658–10666. [PubMed: 31318563]

(36). Dameron AA; Hampton JR; Smith RK; Mullen TJ; Gillmor SD; Weiss PS Microdisplacement Printing. Nano Lett. 2005, 5, 1834–1837. [PubMed: 16159233]

(37). Mullen TJ; Srinivasan C; Hohman JN; Gillmor SD; Shuster MJ; Horn MW; Andrews AM; Weiss PS; Microcontact Insertion Printing. Appl. Phys. Lett 2007, 90, 063114.

(38). Srinivasan C; Mullen TJ; Hohman JN; Anderson ME; Dameron AA; Andrews AM; Dickey EC; Horn MW; Weiss PS Scanning Electron Microscopy of Nanoscale Chemical Patterns. ACS Nano 2007, 1, 191–201. [PubMed: 19206649]

(39). Andrews AM; Liao W-S; Weiss PS Double-Sided Opportunities Using Chemical Lift-Off Lithography. Acc. Chem. Res 2016, 49, 1449–1457. [PubMed: 27064348]

Author Manuscript Author Manuscript Author Manuscript Author Manuscript

(40). Tabaei SR; Jackman JA; Kim S-O; Zhdanov VP; Cho N-J Solvent-Assisted Lipid Self-Assembly at Hydrophilic Surfaces: Factors Influencing the Formation of Supported Membranes. Langmuir 2015, 31, 3125–3134. [PubMed: 25679066]

(41). Silin VI; Wieder H; Woodward JT; Valincius G; Offenhausser A; Plant AL The Role of Surface Free Energy on the Formation of Hybrid Bilayer Membranes. Langmuir 2002, 22, 8163–8168.

(42). Tero R; Takizawa M; Li Y; Yamazaki M; Urisu T Lipid Membrane Formation by Vesicle Fusion on Silicon Dioxide Surfaces Modified with Alkyl Self-Assembled Monolayer Islands. Langmuir 2004, 20, 7526–7531. [PubMed: 15323498]

(43). Arima Y; Iwata H Effects of Surface Functional Groups on Protein Adsorption and Subsequent Cell Adhesion Using Self-Assembled Monolayers. J. Mater. Chem 2007, 17, 4079–4087.

(44). Choi B; Iwanaga M; Miyazaki H; Sugimoto Y; Ohtake A Overcoming Metal-Induced Fluorescence Quenching on Plasmo-Photonic Metasurfaces Coated by a Self-Assembled Monolayer. Chem. Commun 2015, 51, 11470–11473.

(45). Cho N-J; Frank CW; Kasemo B; Höök F Quartz Crystal Microbalance with Dissipation Monitoring of Supported Lipid Bilayers on Various Substrates. Nat. Protoc 2010, 5, 1096–1106. [PubMed: 20539285]

(46). Reimhult E; Höök F; Kasemo B Intact Vesicle Adsorption and Supported Biomembrane Formation from Vesicles in Solution: Influence of Surface Chemistry, Vesicle Size, Temperature, and Osmotic Pressure. Langmuir 2002, 19, 1681–1691.

(47). Sut TN; Jackman JA; Cho N-J Understanding How Membrane Surface Charge Influences Lipid Bicelle Adsorption onto Oxide Surfaces. Langmuir 2019, 35, 8439–8444.

(48). Keller CA; Glassmästar K; Zhdanov VP Kasemo, B. Formation of Supported Membranes from Vesicles. Phys. Rev. Lett 2000, 84, 5443–5446. [PubMed: 10990964]

(49). Jackman JA; Yorulmaz Avsar S; Ferhan AR; Li D; Park JH; Zhdanov VP; Cho N-J Quantitative Profiling of Nanoscale Liposome Deformation by a Localized Surface Plasmon Resonance Sensor. Anal. Chem 2017, 89, 1102–1109. [PubMed: 27983791]

(50). Van Dam L; Karlsson G; Edwards K, Direct Observation and Characterization of DMPC/DHPC Aggregates under Conditions Relevant for Biological Solution NMR. Biochim. Biophys. Acta, Biomembr 2004, 1664, 241–256.

(51). Williams LM; Evans SD; Flynn TM; Marsh A; Knowles PF; Bushby RJ; Boden N Kinetics of the Unrolling of Small Unilamellar Phospholipid Vesicles onto Self-Assembled Monolayers. Langmuir 1997, 13, 751–757.

(52). Lingler S; Rubinstein I; Knoll W; Offenhäusser A Fusion of Small Unilamellar Lipid Vesicles to Alkanethiol and Thiolipid Self-Assembled Monolayers on Gold. Langmuir 1997 13, 7085–7091.

(53). Keller CA; Kasemo B Surface Specific Kinetics of Lipid Vesicle Adsorption Measured with a Quartz Crystal Microbalance. Biophys. J 1998, 75, 1397–1402. [PubMed: 9726940]

(54). Berne BJ; Pecora R Dynamic Light Scattering: With Applications to Chemistry, Biology, and Physics. Courier Corporation: 2000.

Author Manuscript Author Manuscript Author Manuscript Author Manuscript

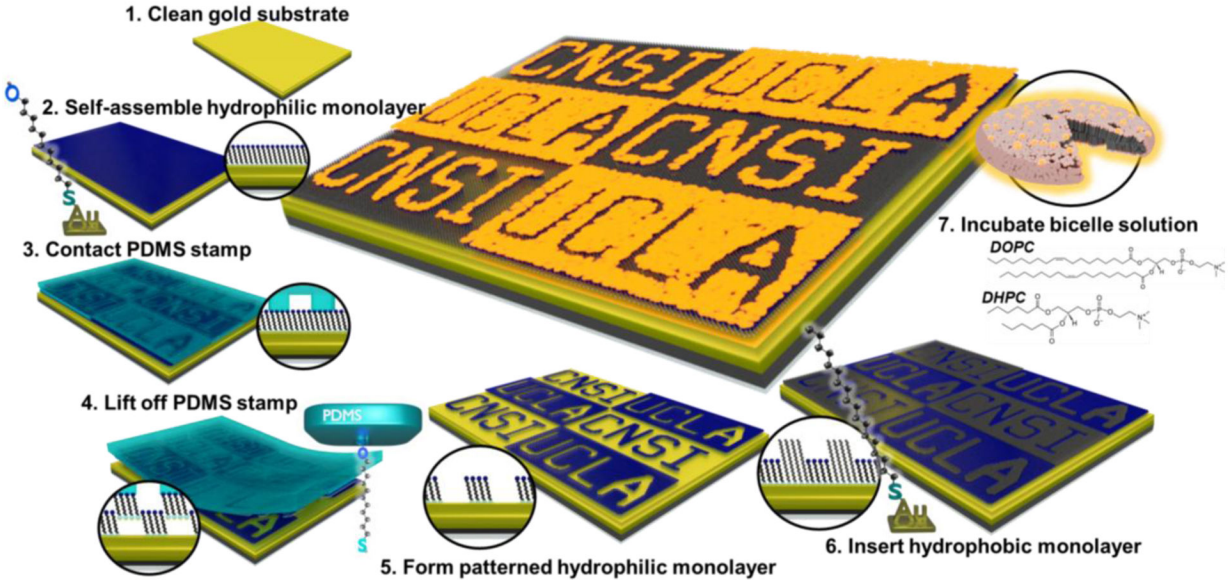

Figure 1. Schematic illustration of lipid bicelle micropatterning using chemical lift-off lithography.

(1) A gold substrate is cleaned using a hydrogen annealing step to ensure no organic impurities are residing on the surface. (2) A hydrophilic mercaptoundecanol (HSC11-OH) self-assembled monolayer (SAM) is adsorbed onto the gold surface *via* incubation. (3) A patterned polydimethylsiloxane (PDMS) stamp is brought into contact with the surface, forming a covalent bond between the PDMS and the contacted HSC11-OH. (4) The contacted molecules are selectively removed by lifting off the PDMS and (5) patterned HSC11-OH resides on the gold surface. (6) A hydrophobic 1-octadecanethiol SAM is inserted into the exposed gold regions, forming a mixed monolayer with contrasting wettability. (7) Bicelles are adsorbed to the patterned hydrophilic regions to form patterned bicelle adlayers.

Author Manuscript Author Manuscript Author Manuscript Author Manuscript

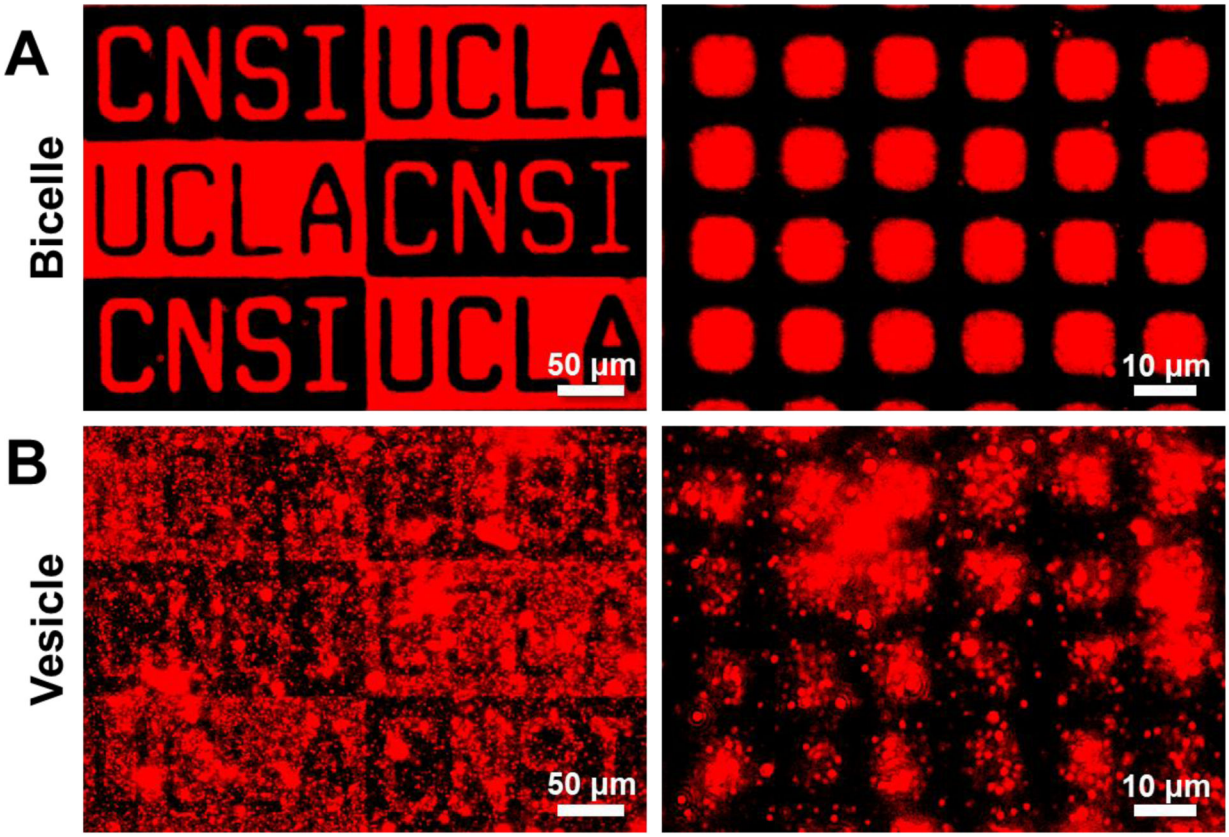

Figure 2. Micropatterning of lipid bicelles and vesicles on chemically functionalized gold surfaces.

Fluorescence micrographs show the results of fluorescently labeled (red) lipid **(A)** bicelle and **(B)** vesicle adsorption onto micropatterned self-assembled monolayer-functionalized gold surfaces consisting of hydrophilic mercaptoundecanol and hydrophobic 1-octadecanethiol with different pattern geometries (UCLA-CNSI and squares). Micrographs are taken after 45 min of incubation and a buffer washing step for each lipid nanostructure.

Author Manuscript Author Manuscript Author Manuscript Author Manuscript

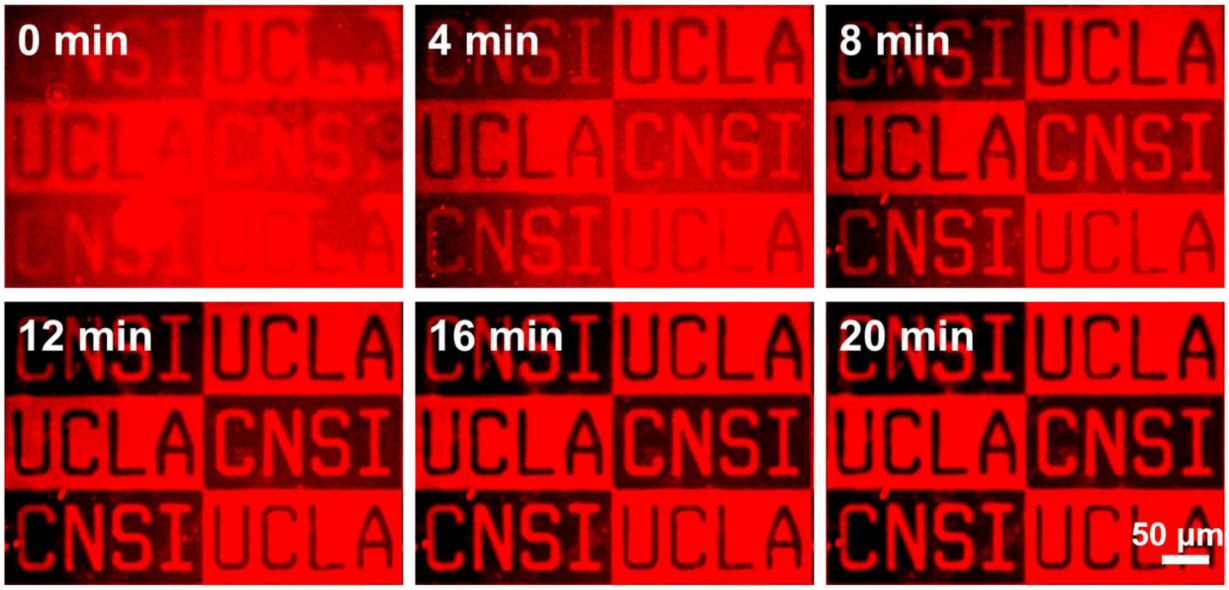

Figure 3. Time-lapse fluorescence microscopy imaging of lipid bicelle adsorption onto a micropatterned gold surface.

Fluorescence micrographs of fluorescently labeled lipid bicelles incubated with a post-chemical lift-off lithography mixed SAM-functionalized gold surface consisting of hydrophilic mercaptoundecanol and hydrophobic 1-octadecanethiol. The mixed monolayer surfaces are incubated in the fluorescently-labeled bicelle solution and images are taken sequentially to avoid bleaching the fluorophore. Bicelle patterning was first observed at $t = 0$ min, and image snapshots of the surface are presented for every 4 min after incubation started. After 20 min of incubation, bicelles are preferentially adsorbed to the hydrophilic SAM regions. For all images, there was no wash step in order to observe the bicelle adsorption behavior.

Author Manuscript Author Manuscript Author Manuscript Author Manuscript

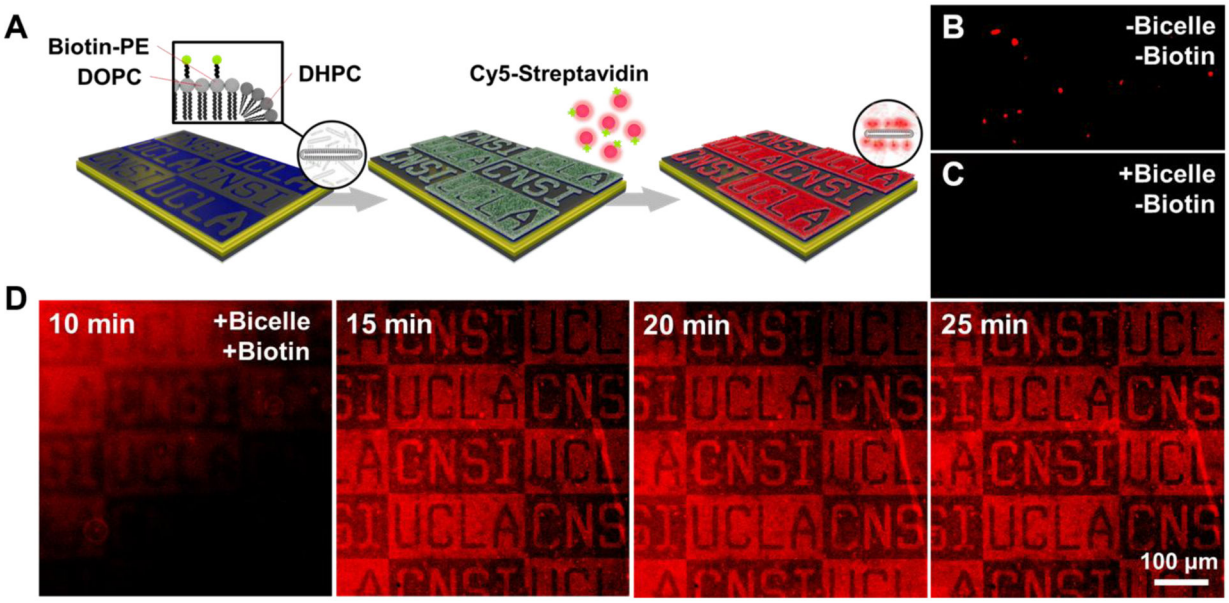

Figure 4. Selective protein binding to micropatterned lipid bicelles.

(A) Schematic illustration of fluorescently labeled streptavidin binding to predefined bicelle patterns that were previously adsorbed to mixed-monolayer functionalized gold surfaces. The bicelles consist of biotinylated-lipid compositions consisting of 1,2-dioleoyl-*sn*-glycero-3-phosphocholine (DOPC), 1,2-dihexanoyl-*sn*-glycero-3-phosphocholine (DHPC), and 1,2-dioleoyl-*sn*-glycero-3-phosphoethanolamine-*N*-(cap biotinyl) (Biotin-PE). Fluorescence micrographs depict negligible streptavidin binding to **(B)** chemically functionalized gold surface without bicelle coating and **(C)** micropatterned lipid bicelles without biotinylated lipid. **(D)** Fluorescence micrographs show time-lapse image snapshots of streptavidin binding to biotinylated lipid-functionalized bicelle patterns. Streptavidin was added at $t = 0$ min and incubated for 25 min. For all images, there was no wash step in order to observe the binding behavior of fluorescently labeled streptavidin.

Author Manuscript Author Manuscript Author Manuscript Author Manuscript

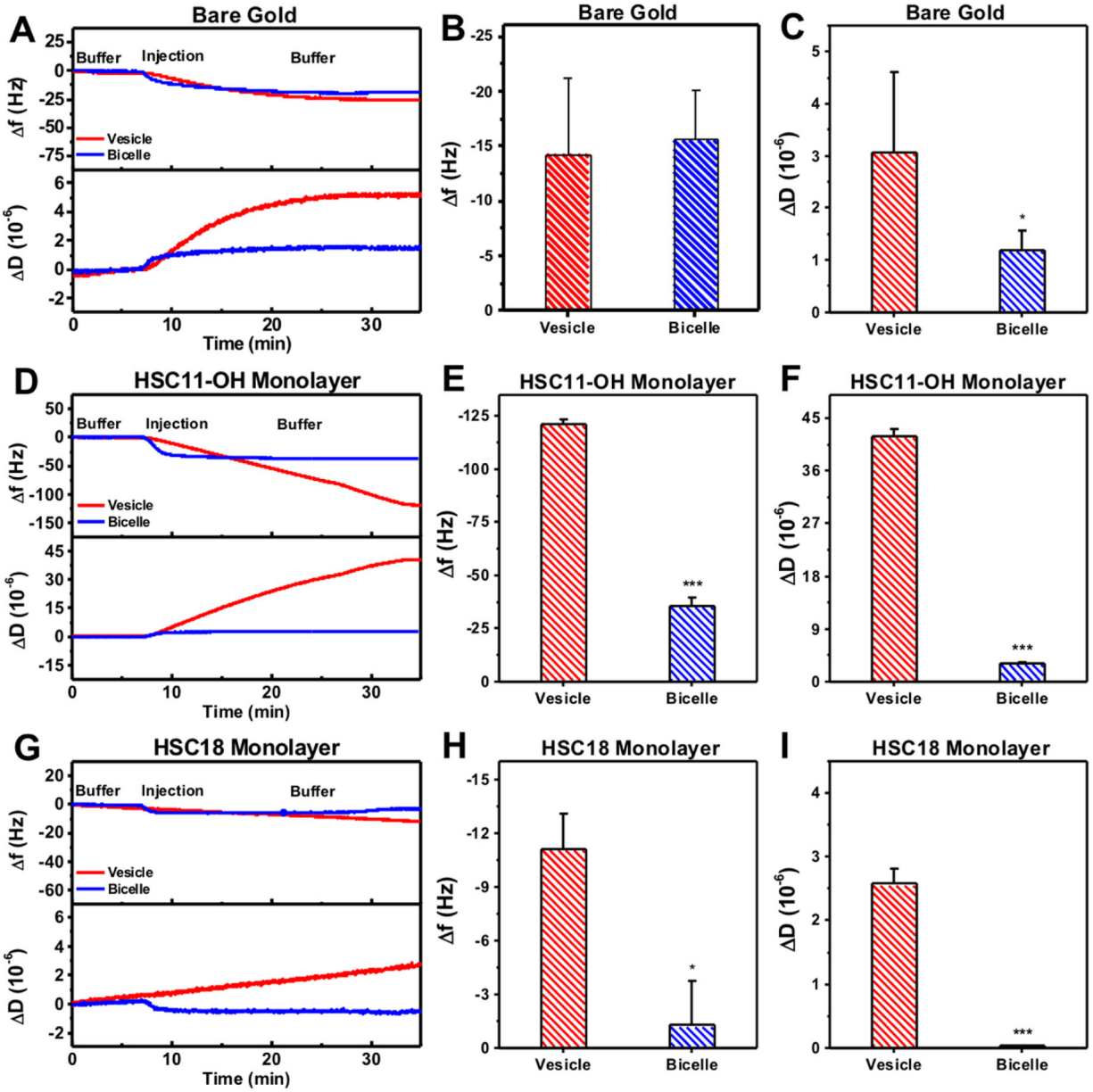

Figure 5. Quartz crystal microbalance and dissipation (QCM-D) characterization of lipid bicelle and vesicle adsorption onto bare, mercaptoundecanol (HSC11-OH), and 1-octadecanethiol (HSC18)-functionalized gold surfaces.

(A) QCM-D Δ*f* and dissipation (ΔD) shifts as a function of time for lipid bicelle and vesicle adsorption onto bare gold surfaces. **(B)** Magnitude of final Δf and **(C)** ΔD shifts corresponding to data in panel (A). **(D)** QCM-D Δ*f* and ΔD shifts as a function of time for lipid bicelle and vesicle adsorption onto HSC11-OH-functionalized gold surfaces. **(E)** Magnitude of final Δ*f* and **(F)** ΔD shifts corresponding to data in panel. **(G)** QCM-D Δ*f* and ΔD shifts as a function of time for lipid bicelle and vesicle adsorption onto HSC18-functionalized gold surfaces. Magnitude of final **(H)** Δ*f* and (**I**) ΔD shifts corresponding to data in panel (G). Data are expressed as mean ± standard error of the mean for $n = 4$ runs,

Author Manuscript Author Manuscript Author Manuscript Author Manuscript

and statistical significance was determined by using the Student's t-test (*p<0.05, **p<0.01, and ***p<0.001).